International Journal of Theoretical Physics, Vol. 42, No. 10, October 2003 (© 2003)

Resonances: Calculations and Observables

L. S. Ferreira[1,4] and E. Maglione[2,3]

Received June 30, 2003

Methods to calculate resonances energies, decay widths, and corresponding wave functions, are discussed in realistic problems. Proton radioactivity from deformed drip-line nuclei described as decay of a resonant state of the proton in the field of the daughter nucleus, is used to test the models and to show that all experimental data currently available can be consistently described.

KEY WORDS: resonances; calculations; observables.

1. INTRODUCTION

Resonances are one of the most interesting phenomena in many fields of physics which lead to important findings. In the quantum world, systems with electrons, hadrons, or atoms provide enormous amount of data on resonances, leading to the discovery of new states of matter. In nuclear physics, the recent findings on proton radioactive nuclei (Woods and Davis, 1997), added to the list many new examples, which are important not only as direct data on resonances, but also for the production in the laboratory of new isotopes, in regions of the nuclear chart which were "terra incognita," until recently. In fact, the latest research activity in nuclear radioactivity, aims to produce exotic nuclei with proton or neutron excess and reach the limits of stability of matter, known as drip-lines, beyond which a nucleon is no more bound, but can stay as a resonance. We are still far in research capability to reach the neutron drip-line, since it is still impossible to produce in the lab the heavy elements that by fragmentation could reach the limit of neutron excess, but the same is not true for protons. The recent studies (Woods and Davis, 1997) of proton radioactivity from spherical and deformed nuclei, have almost

[1] Centro de Física das Interacções Fundamentais and Departmento de Física, Instituto Superior Técnico, Lisboa, Portugal.
[2] Dipartimento di Fisica "G. Galilei," Padova, Italy.
[3] INFN, Sezione di Padova, Italy.
[4] To whom correspondence should be addressed at Centro de Física das Interacções Fundamentais and Departamento de Física, Instituto Superior Técnico, Av. Rovisco Pais, P-1049-001 Lisboa, Portugal; e-mail: flidia@ist.utl.pt.

0020-7748/03/1000-2117/0 © 2003 Plenum Publishing Corporation

completely defined the proton drip-line for $50 < Z < 82$. What is really observed is the emission of a proton out of a nucleus just in the vicinity of the drip-line, beyond it, where the proton forms a resonant state in the field of the daughter nucleus. In order to escape it has to tunnel through the Coulomb and centrifugal barriers which are quite long, of the order of 10–20 times the nuclear radius, therefore the decay widths of these resonances are very narrow of the order of 10^{-16}–10^{-22} MeV. The escape energy of the emitted proton is also very small, around 1 MeV, therefore these resonances lie very low in the continuum, and correspond essentially to single particle excitations. Most part of the proton emitters are spherical, but there are also examples showing quite large deformations, therefore, the single particle states have to be known in a field with a specific shape.

The observables that are measured experimentally are the energy of the emitted proton and the half-life for decay of the resonance. Through the reaction mechanisms for their emission, it is possible to learn about the structure of the elements that form these resonances. Therefore, in order to sort out the nuclear structure properties of these decaying nuclei from kinematics, very precise calculations of these resonances have to be performed to be able to reproduce the experimental data.

The study of realistic problems as discussed above, requires adequate interactions, and always leads to the solution of complicated coupled channel equations. It is the aim of this work, to discuss how to calculate the wave functions and the half-lives of resonances in such cases. Realistic examples are provided by proton drip-line nuclei, and it is shown how it is possible with our formalism, to interpret perfectly the existing data on these exotic nuclei.

2. RESONANCES IN COUPLED CHANNEL PROBLEMS

In proton radioactive nuclei with an odd number Z of protons, and even number N of neutrons, the emitted odd nucleon can be considered moving in a single particle level, which corresponds to a resonance of the unbound core-proton system. Therefore, the problem can be described by the radial Schrödinger equation for the mean field felt by the nucleons moving in the nucleus, whose solution corresponds to the single particle state. The equation should then be solved (Ferreira *et al.*, 1997) imposing regularity at the origin and outgoing wave boundary conditions at large distance for each partial wave, as required for resonances, i.e.,

$$\lim_{r\to\infty} R_{ljm}(r) = N_{ljm}(G_l(kr) + iF_l(kr)), \tag{1}$$

to find the resonance states. The functions F and G are the regular and irregular Coulomb functions, $k = \sqrt{2\mu E/\hbar^2}$ the wave number, and N_{ljm} a normalization constant.

In general, the nuclear surface is not spherical, since rotational spectra has been observed in many nuclei. Deformation is usually described by parameterizing the nuclear radius in terms of a multipole expansion on spherical harmonics $Y_{\lambda,\mu}$, depending on a set of deformation parameters $\hat{\beta}$ that represent variations in relation to a standard spherical shape. The spherical case is automatically taken into account by setting $\beta = 0$. The quadrupole axially symmetric deformation is given by the term with $\lambda = 2$, $\mu = 0$, and is in general the most important contribution to deformation. The corresponding parameter $\beta_2 \equiv \beta$ can be positive or negative according to a prolate or oblate form of the nucleus.

The nucleus is then viewed as a system of independent particles moving in a deformed mean field. It is still an open problem to derive the nuclear mean field from a microscopic approach, starting from the bare interaction between the nucleons. Pure phenomenological shapes have to be adopted, that include a central part, spin–orbit term, and the Coulomb interaction for the deformed charge distribution. The central term is represented by a deformed Woods–Saxon potential, of the form,

$$V(\vec{r}, \hat{\beta}) = \frac{V_0}{1 + \exp[dist_{\sum}(\vec{r}, \hat{\beta})/a]}, \tag{2}$$

where $dist_{\sum}(\vec{r}, \hat{\beta})$ is the distance between the point $\vec{r}$ and the nuclear surface, a the diffuseness parameters, and V_0 the strength. The deformed spin orbit potential is assumed to be,

$$V_{ls} = \lambda \left(\frac{\hbar}{2Mc}\right)^2 \left\{\Delta \frac{V_0}{1 + \exp[dist_{\sum}(\vec{r}, \hat{\beta})/a_{ls}]}\right\} \cdot (\vec{\sigma} \times \vec{p}), \tag{3}$$

with λ the strength of the spin–orbit interaction, and M and σ are the mass and spin of the nucleon, respectively.

The previous expressions to describe the interaction, depend on strength, radius, and diffuseness parameters that are adjusted to reproduce single particle properties of deformed nuclei. Due to inherent potential ambiguities and fits to different compilations of data, there are various sets of parameters that differ somewhat amongst each other. It is well known that predictions from this type of interactions are most sensitive to the surface region, and it is possible to find several combinations of strength and geometry parameters that give the same results. The earliest parameterizations date from the 60s and fit stripping and pickup data on spherical nuclei for the sp energies, mainly on ^{208}Pb, and lighter nuclei. Since then, the range of experimental data has been enlarged considerably, and other observables, like ground state spins and parities, on spherical and deformed odd-mass nuclei, and ground state equailibrium deformations were simulataneously taken into account. For example, the "universal parameters" (Cwiok *et al.*, 1987), are valid throughout the periodic table including extensions to exotic nuclei, and describe quite well single particle level sequences and nuclear equilibrium deformations. From the

work done in this field, it is possible to confirm that the deformed Woods–Saxon is quite adequate to describe nuclear properties, but small changes in the parameters of the spin–orbit interaction play a decisive role in getting the correct order and distance between the levels. For details see Ferreira *et al.* (2002).

Assuming that the system has axial symmetry, the wave function $\Psi(\vec{r})$, that satisfies the time independent Schrödinger equation, can be expanded in spherical waves, i.e.

$$\Psi_m(\vec{r}) = \sum_{lj} R_{ljm}(r)[Y_l(\omega)\chi]_{jm} \tag{4}$$

since m is a conserved quantity, R_{ljm} are the radial functions, χ the spin function, and the square parenthesis indicate the coupling of angular momentum and spin to a final state jm. Projecting the Schrödinger equation on the angular and spin part $[Y_{l'}(\omega)\chi]_{j'm}$ one obtains a set of coupled channel radial differential equations which has the form,

$$\left(\frac{d^2}{dr^2} + k^2 - \frac{l(l+1)}{r^2}\right) R_{ljm}(r) = \frac{2m}{\hbar^2} \sum_{l'j'} \left(V^m_{1ljl'j'} + V^m_{2ljl'j'} \frac{d}{dr}\right) R_{l'j'm}(r) \tag{5}$$

where the quantities $V^m_{1\alpha\alpha'}$ and $V^m_{2\alpha\alpha'}$ are the matrix elements of the interaction taken between the angular and spin parts of the partial waves, depending on r, and α designates the set of quantum numbers lj. The first derivative of the wave function is coming from the deformed spin–orbit potential.

The solution of these coupled channel equations for such interactions, is complicated. The deformed spin–orbit part of the potential, represented by a first order derivative term, brings extra difficulties to the numerical solution of the equation, and some mathematical transformations are needed as discussed in Ferreira *et al.* (1997) to have stable and very precise solutions needed for comparison with the experimental data. However it is possible to get solutions with great accuracy, and determine the resonance energies and wave functions for each deformation β.

2.1. Exact Calculations

In general, a set of N coupled differential equations of second order like Eqs. (5) can be cast in the form,

$$H\mathcal{R} = E\mathcal{R} \tag{6}$$

where $\mathcal{R}$ is a vector. They can be solved in principle, integrating with N linearly independent initial conditions for the function and its derivatives, and construct with the solutions, a matrix $\bar{\mathcal{R}}$ of N column vectors such that the true wave function can be expressed as a linear combination of them, propagated from the origin and

from large distances up to a matching radius r_m. This can be expressed as,

$$\mathcal{R}(r) = \bar{\mathcal{R}}(r)^+ c^+ r \leq r_m$$
$$\mathcal{R}(r) = \bar{\mathcal{R}}(r)^- c^- r \leq r_m \tag{7}$$

where the $\pm$ sign designates that the wave function matrices were propagated from short and long range, and $c^\pm$ are r-independent column vectors to be found. Imposing continuity of the wave function and derivative at the matching point r_m, one gets,

$$\bar{\mathcal{R}}(r_m)^+ c^+ = \bar{\mathcal{R}}(r_m)^- c^-$$
$$[\bar{\mathcal{R}}(r_m)^+]' c^+ = [\bar{\mathcal{R}}(r_m)^-]' c^-. \tag{8}$$

These equations are equivalent to a $2N \times 2N$ system of homogeneous and linear equations with nontrivial solution only if the determinant of the matrix is zero. Propagation of the wave function in the classically forbidden region is numerically unstable. In this region, the exponentially growing solutions in locally closed channels of large 1 dominate the matrix, and destroy the linear independence leading to a loss of accuracy. If instead, the equations are written in terms of the log derivative of the wave function, the propagation of the wave functions is numerically stable. Therefore, we have considered the matrix

$$\Phi^m(r) = \left[\frac{d}{dr}\bar{\mathcal{R}}_m(r)\right] \times \bar{\mathcal{R}}_m^{-1}(r), \tag{9}$$

and written Eq. (5) as,

$$\frac{d}{dr}\Phi^m_{\alpha\alpha'}(r) - \sum\nolimits_{\alpha''} V^m_{2\alpha\alpha''}\Phi^m_{\alpha''\alpha'}(r) + \sum\nolimits_{\alpha''} \Phi^m_{2\alpha\alpha''}(r)\Phi^m_{\alpha''\alpha'}(r)$$
$$+ \left[k^2 - \frac{l_\alpha(l_{\alpha+1})}{r^2}\right]\delta_{\alpha,\alpha'} - V^m_{1\alpha\alpha'} = 0. \tag{10}$$

The Schrödinger equation is thus transformed in a nonlinear matrix differential equation of first order with $N \times N$ equations which have to be integrated only once. The multichannel matching conditions are expressed in terms of Φ^m,

$$\Phi^m(r_m)^+ \mathcal{R}(r_m) = \Phi^m(r_m) - \mathcal{R}(r_m) \tag{11}$$

which has a non trivial solution only if the determinant $\|\Phi^m(r_m)^+ - \Phi^m(r_m)^-\|$ of the matrix is zero. If E is an eigenvalue, a vector state $\mathcal{R}$ must exist fulfilling this condition. Therefore, finding the eigenvalue corresponds to finding the zero of the determinant and the method is very stable. Equations (11) form in principle an infinite set which has to be truncated in practical applications. The choice of the number of terms to keep, which is equivalent to select a limiting angular momentum, is determined by the accuracy required.

Following this procedure, the energy solutions of the Schrödinger equation were determined. For real, negative energies one gets normalized wave functions, with the proper exponentially decreasing tail, in correspondence to the energy eigenvalues of the bound system. For resonances, on the other hand, one gets purely outgoing states with complex eigenvalues $E_R - i\Gamma/2$ which have automatically an imaginary part, related to the decay width of the resonance they describe. The normalization of these unbound wave functions is given by the standard Zel'dovich (Zel'davich, 1961) regularization. Deformation appears as a parameter, therefore the equations have to be solved for each value of β.

It is very interesting to study the behavior of these resonances in the complex plane, as a function of β. This is shown in Fig. 1 for ^{113}Cs. At zero deformation the nucleus is spherical and the states are specified by the usual shell model quantum numbers $[lj]$ and parity π. Switching on β, the total angular momentum is not any more a conserved quantity, but its projection "m" on the z-axis is a conserved

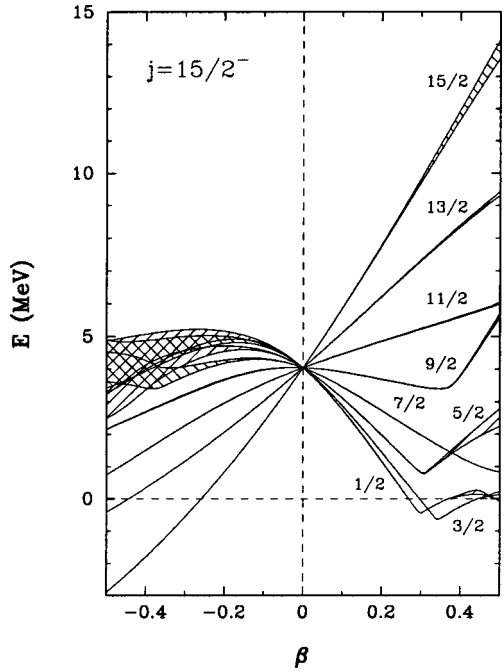

Fig. 1. Real part of the energy as a function of the deformation β of all deformed neutron states coming from the spherical level $j15/2^-$ in ^{113}Cs. The corresponding "m" values are given. For states that lie in the continuum two lines are drawn, and the distance between them (shadowed area) correspond to half of the resonance width.

quantity. Varying β, the states split into their "m" components, and it is possible to study their energy dependence with deformation.

There are drastic changes of the position in the plane, according to the value of the deformation. Resonances can attract or repel each other, or even become bound states. This has very interesting consequences in a real system. In a specific nuclear isotope, a certain deformation can still bind a nucleon, unbound for other value of β, or make a resonance very narrow, which is an experimentally observable quantity. Exotic nuclei are certainly candidates for this phenomena, therefore these studies can have an important predicting power.

2.2. Analytic Continuation in the Coupling Constant

Resonance energies and wave functions can also be obtained by means of Analytic Continuation in the Coupling Constant to weaker binding. The method, proposed long ago by Kukulin and co-workers (Kukulin *et al.*, 1979; Kukulin and Krasnopol'sky, 1977) is based on the fact that for an attractive potential V, with a strength parameter of the type λV, a resonance state will become a bound state as the coupling strength is increased. It is possible to prove (Kukulin *et al.*, 1979; Kukulin and Krasnopol'sky, 1977) that the wave number $k = \sqrt{2\mu E}/\hbar$ is an analytic function of the strength λ and around the threshold $k\,(\lambda_0) = 0$, one has

$$k(\lambda) \sim i\sqrt{\lambda - \lambda_0} \tag{12}$$

for any l, taking into account the Coulomb interaction. These properties suggest the analytic continuation of k in the complex λ-plane from the bound-state region into the resonance region through the employment of Padé approximants of the second kind,

$$k \simeq k^{(N,M)}(x) = i\,\frac{c_0 + c_1 x + c_2 x^2 + \cdots + c_M x^m}{1 + d_1 x + d_2 x^2 + \cdots + d_N x^N}, \tag{13}$$

where $x \equiv \sqrt{\lambda - \lambda_0}$. In practice, one solves the bound-state problem for λV in correspondence to $N + M + 1$ different values λ_i of the coupling strength. Given the threshold value λ_0, the $N + M + 1$ coefficients in the Padé approximants can be determined by equating $k^{(N,M)}(x_i)$ to the actual values k_i of the wave number. The approximants can then be used to estimate the resonance wave number k_r, and hence the resonance position and width, in correspondence to the "physical value" $\lambda = 1$ of the potential strength. A similar procedure (Cattapan and Maglione, 2000) can be used in the complex k-plane to analytically continue the bound-state wave function $\psi_l^{(B)}(r)$ into the scattering region for any value of the radial variable r.

The method was applied to the proton emitter ^{131}Eu and is illustrated in Fig. 2. The real part of the energy of the $m = 3/2+$ state in shown as a function of λ. The Padé extrapolation was obtained starting from the bound-state region, for

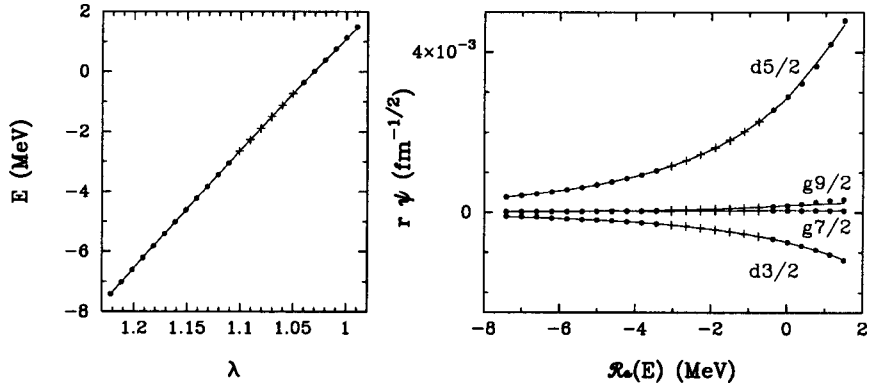

Fig. 2. Energy eigenvalue and wave function for the proton $3/2+$ state in ^{131}Eu. The dominat wave-function components $r\psi_{lj}(r)$ are evaluated at $r = 15$ fm. The full dots represent the results obtained from the numerical solution of the Schrödinger equation, whereas crosses are the input values used for the analytic continuation. Full curves are the outcome of the Padé extrapolation.

different decreasing values of the coupling strength. The relevant wave-function components at $r = 15$ fm for decay from the $m = 3/2+$ state, are given in the right panel of Fig. 2.

A rather low-rank (3,3) Padé approximant can reproduce extremely well the exact results, and the method can be confidently applied to these situations, where high numerical accuracy is required in order to have a meaningful comparison with the experimental data.

3. CALCULATION OF DECAY WIDTHS

There are different models to calculate decay widths for proton decay from odd-Z even N nuclei. This quantity, can be determined from the imaginary part of the energy that solves the Schrödinger equation for resonances, but a great numerical precision is needed for such small half-lives of few ms that correspond to widths of $\approx 10^{-20}$ MeV.

The half-lives can also be obtained by noticing that the partial decay width is the overlap between the initial and final states (Humblet and Rosenfeld, 1961). The wave function of the parent nucleus can be considered as the function of a particle plus a rotor, identified with the daughter nucleus, in the strong coupling limit (Bugrov *et al.*, 1990; Bugrov and Kadmenskii, 1989). In this approach, the partial decay width can be written as,

$$\Gamma^{J_d}_{l_p j_p} = \frac{\hbar^2 k}{\mu} \frac{(2J_d+1) < J_d, 0, j_p, K_i | K_i >^2}{K_i + 1/2} |N_{l_p j_p K_i}|^2 u^2 K_i, \qquad (14)$$

where the total momentum of the initial and daughter nucleus K_i and J_d, are related to the one of the escaping proton by the relation $J_d + K_i \geq j_p \geq M_{\text{Max}}(K_i, |J_d - K_i|)$. The quantity $u^2_{K_i}$ is the probability that the single particle level in the daughter nucleus is empty, evaluated in the BCS approach. Aside from angular momentum recoupling coefficients, the decay width of Eq. (8) is completely defined by the asymptotic normalization N. The most important contribution to the asymptotic normalization comes from the real part of the wave function, which is determined with great precision.

In most cases, decay occurs mainly to the ground state of the daughter nucleus, so $J_d = 0$, and the outgoing proton has the largest possible energy. Its momentum is then equal to the total and initial momentum of the daughter nucleus, $j_p = J_i = K_i$. There is only one component of the wave function that contributes. In the case of decay to excited states, few combinations are permitted for $l_p j_p$ according to angular momentum coupling rules, and consequently different components of the parent wave function are then tested. It is possible that decays to different states are allowed, and a total width Γ_T should be defined as the sum of all partial widths satisfying Eq. (14), and branching ratios as the ratio between partial and total widths.

The decay width obtained from Eq. (14) depends on deformation, and is very sensitive to the wave function of the decaying state. Therefore, if it is able to reproduce the experimental value, will give clear information on the deformation and properties of the decaying state.

As an example we have chosen ^{131}Eu, a well deformed proton emitter with a predicted quadrupole deformation $\beta_2 = 0.33$ (Moller *et al.*, 1995, 1997). Two proton lines were observed (Sonzogni *et al.*, 1999) in the decay of this element, at 932(7) keV with half-life $T_{1/2} = 17.8(19)$ ms corresponding to the ground state proton decay, and at 811(7) keV with $T_{1/2} = 23^{10}_{-6}$ ms. Since these two half-lives are very similar, the second line was interpreted as decay to the excited 2^+ state in ^{130}Sm with a branching ratio of 0.24 ± 0.05 and a total half-life of $T_{1/2} = 20.2(25)$ ms.

The single particle levels, bound states and resonances, were determined from the exact solution of Eq. (5), and are shown in Fig. 3. The states close to the Fermi level, are the decaying ones, since the parent nucleus is in the ground state. For them the half-lives for decay were calculated making use of Eq. (14), and are also presented in Fig. 3, in comparison with the experimental results. The states $K = 5/2^+_a$, $K = 3/2^-$, and $K = 3/2^+$, could describe the half-life for decay. The first state, describes it with β in the range of 0.15–0.28, whereas the other two in the range of 0.2–0.24 and 0.24–0.34, respectively. Since experiment provides extra information, the calculation of the branching ratio shown in Fig. 4, permits to eliminate the states $K = 5/2^+_a$ and $K = 3/2^-$, which predict a branching ratio one order of magnitude smaller than the experimental value. Therefore, the interpretation of the fine structure data, allows an unambiguous determination

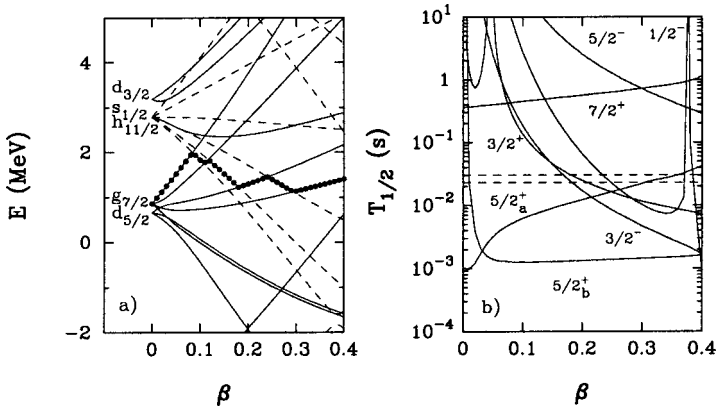

Fig. 3. a) Proton single particle Nilsson levels of ^{131}Eu. The dotted lines indicate the Fermi level. b) Half-lives of the resonances of ^{131}Eu, as function of deformation β, (full lines), for levels close to the Fermi energy. The shadowed area represents the uncertainty due to the experimental error on the energy of the proton. The experimental value, that lies between the dashed lines, is taken from Sonzogni *et al.* (1999).

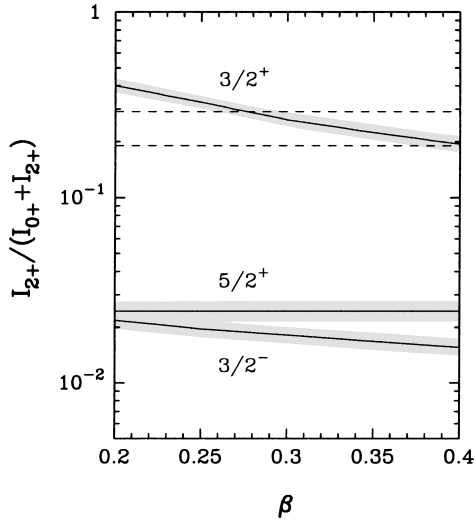

Fig. 4. Branching ratio for the decay to the 2^+ state of ^{130}Sm as a function of deformation.

of the angular momentum, $K = 3/2^+$ and deformation $\beta \approx 0.27$, of ^{131}Eu, in agreement with predictions of Möller *et al.* (1995, 1997).

The decay of the remaining measured odd–even deformed emitters, ^{109}I, ^{113}Cs, ^{141}Ho, ^{151}Lu, and the just found ^{117}La (Soramel *et al.*, 2001), and the isomeric decays of ^{141m}Ho, ^{151m}Lu, and ^{117m}La, were also perfectly understood (Maglione and Ferreira, in press) within this model.

Emission from deformed systems with an odd number of protons and neutrons can be discussed in a similar fashion (Ferreira and Maglione, 2001). The decaying nucleus is described by a wave function of two particles-plus-rotor in the strong coupling limit represented in terms of the single particle functions of the odd nucleons. However, in contrast with decay to ground state of odd–even nuclei where the proton is forced to escape with a specific angular momentum, many channels will be open due to the angular momentum coupling of the proton and daughter nucleus, $\vec{J}_d + \vec{J}_p$, giving a total width for decay as a sum of partial widths allowed by parity and momentum conservation,

$$\Gamma^{J_d} = \sum_{j_p=\max(|J_d-K_T|,K_p)}^{J_d+K_T} \Gamma^{j_d}_{l_p j_p} \tag{15}$$

where the width for decay in the channel $l_p j_p$ is given by,

$$\Gamma^{j_d}_{l_p j_p} = \frac{\hbar^2 k}{\mu} \frac{(2J_d+1)}{(2K_T+1)} \langle J_d, K_n, j_p, K_p | K_T, K_T \rangle^2 \times \frac{|u_{l_p j_p}(r)|^2}{|G_{l_p}(kr) + i F_{l_p}(kr)|^2} u^2 K_p. \tag{16}$$

The factor $u^2_{K_p}$ is the probability that in the daughter nucleus the proton single particle level is empty, evaluated with the pairing interaction in the BCS approach. The quantity in brackets represents a Clebasch–Gordan resulting from the angular momentum coupling of the odd nucleons, and $K_T = |K_p \pm K_n|$ the spin of the bandhead state of the decaying nucleus. Since the neutron intrinsic state does not change during decay $K_d = K_n$. The total decay width depends on the quantum numbers of the unpaired neutron which cannot be considered only a spectator, but contributes significantly with its angular momentum to the decay. The proton and neutron single particle Nilsson levels in ^{112}Cs are depicted in Fig. 4 as a function of deformation. The neutron.

Fermi level is at levels with $K_n = 1/2^{\pm}, 3/2^+$, or $5/2^+$ according to the deformation value, whereas for protons we took $K_p = 3/2^+$ since it reproduces the decay of ^{113}Cs (Maglione *et al.*, 1998). The corresponding half-lives evaluated from Eqs. (15) and (16), are shown in Fig. 5. They are displayed separately in the two possible coupling cases $K_T = K_p \pm K_n$. Since in each coupling the neutron single particle level leads to quite different factors and intermediate partial widths, the half-lives that depend strongly on these quantities are quite different. The

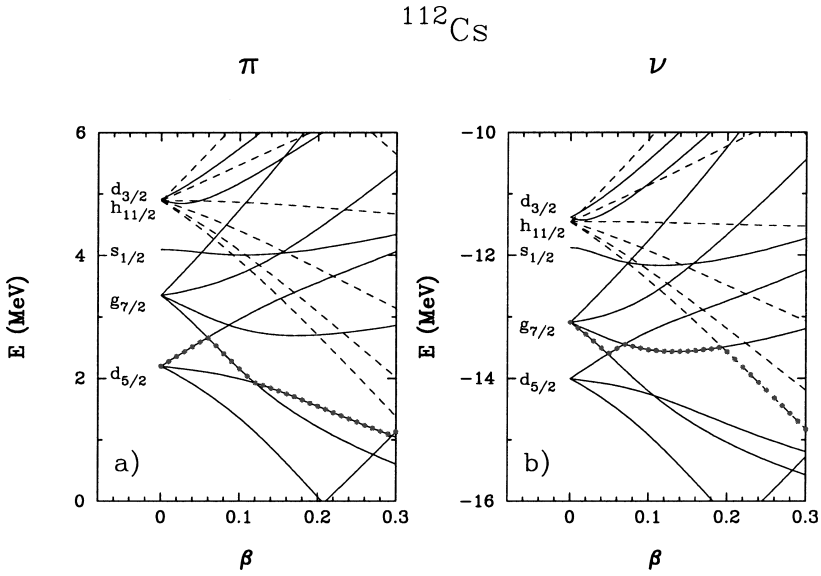

Fig. 5. a) Proton Nilsson levels in ^{112}Cs. The dotted lines denote the levels around the Fermi surface. b) The same as in a) for neutrons.

experimental value is reproduced considering the odd neutron in states with $K_n = 3/2^+, 5/2^+$, with corresponding deformations $\beta > 0.1$ with $K_T = 3^+$, and $\beta > 0.2$ with $K_T = 4^+$, respectively. When the proton and neutron are antiparallel, the same neutron states give $\beta > 0.14$ and $\beta > 0.24$ for $K_T = 0^+, 1^+$, respectively, whereas the $1/2^\pm$ states always have a very long lifetime. The state $K_n = 5/2^-$, should be excluded, since it is the Fermi level only at very low deformation, giving a quite short half-life. Therefore, the only possibility is given by $K_n = 3/2^+$, which is the Fermi level for $0.05 < \beta < 0.19$, and reproduces the experimental half-life in this range of deformations. These deformations are consistent with the ones obtained for ^{113}Cs (Maglione *et al.*, 1998), giving further support to this calculation.

All the other measured odd–odd deformed proton emitters, ^{140}Ho, ^{150}Lu, and the isomeric decay of ^{150m}Lu, were analyzed in a similar way (Maglione and Ferreira, in press), and it was also possible to interpret the data on half-lives identifying completely the decaying state and assigning to the nucleus a deformation compatible with other nuclear structure calculations (Möller *et al.*, 1995, 1997).

4. CONCLUSIONS

The resonance states and their corresponding half-lives for decay are evaluated for a deformed system described by realistic interactions. The eigenstates

are calculated by solving the coupled channel Schrödinger equation for an axially deformed Woods–Saxon potential with outgoing boundary conditions. We have shown how to obtain an exact solution of this complicated coupled channel problem.

An alternative approach was also discussed, by varying the interaction coupling strength so as to analytically continue a bound-state energy eigenvalue, and wave function into the positive energy region, becoming a resonance. Very accurate results were obtained with this approach.

The application of these methods to describe all available experimental data on even–odd and odd–odd deformed proton emitters from the ground and isomeric states, as well as the data on fine structure, was very successful. All observables were accurately and consistently reproduced, identifying the level and deformation of the decaying nucleus, and also supporting previous predictions made by other models on their nuclear structure properties. We have thus shown a very interesting application of the basic theory of resonances, that gave a valuable contribution to the understanding of a class of events in contemporary nuclear physics.

ACKNOWLEDGMENTS

We thank Professor Arno Bohm and Professor Manolo Gadella for the kind invitation to participate at the Jaca meeting. This work was supported by the Fundação de Ciência e Tecnologia (Portugal), Project: POCTI-36575/99.

REFERENCES

Bogdanov, D. D., Bugrov, V. P., and Kadmenskii, S. G. (1990). *Soviet Journal of Nuclear Physics* **52**, 229.

Bugrov, V. P. and Kadmenskii, S. G. (1989). *Soviet Journal of Nuclear Physics* **49**, 967.

Cattapan, G. and Maglione, E. (2000). *Physical Review C: Nuclear Physics* **61**, 67301.

Cwiok, S., Dudek, J., Nazarewicz, W., Skalski, J., and Werner, T. (1987). *Computers in Physics Communications* **46**, 379.

Ferreira, L. S. and Maglione, E. (2001). *Physical Review Letters* **86**, 1721.

Ferreira, L. S., Maglione, E., and Fernandes, D. E. P. (2002). *Physical Review C* **65**, 024323.

Ferreira, L. S., Maglione, E., and Liotta, R. J. (1997). *Physical Review Letters* **78**, 1640.

Humblet, J. and Rosenfeld, L. (1961). *Nuclear Physics* **26**, 529.

Kukulin, V. I. and Krasnopol'sky, V. M. (1977). *Journal of Physics A: Mathematical General* **10**, L33.

Kukulin, V. I., Krasnopol'sky, V. M., and Miselkhi, M. (1979). *Soviet Journal of Nuclear Physics* **29**, 421.

Maglione, E. and Ferreira, L. S. (in press). *European Physics Journal A*.

Maglione, E., Ferreira, L. S., and Liotta, R. J. (1998). *Physical Review Letters* **81**, 538.

Maglione, E., Ferreira, L. S., and Liotta, R. J. (1999). *Physical Review C* **59**, R589.

Möller, P., Nix, J. R., and Kratz, K. L. (1997). *Atomic Data Nuclear Data Tables* **66**, 131.

Möller, P., Nix, J. R., Myers, W. D., and Swiatecki, W. J. (1995). *Atomic Data Nuclear Data Tables* **59**, 185.

Page, R. D. *et al.* (1994). *Physical Review Letters: Nuclear Physics* **72**, 1798.

Sonzogni, A. A. *et al*. (1999). *Physical Review Letters* **83**, 1116.
Soramel, F. *et al*. (2001). *Physical Review C* **63**, 031304(R).
Woods, P. J. and Davids, C. N. (1997). *Annual*. *Review of Nuclear Particle Science* **47**, 541, and references therein.
Zel'dovich, Y. B. (1961). *Soviet Physics JETP* **12**, 542.